AD_____

AWARD Number: W81XWH-11-1-0743

TITLE: Regenerative Medicine for Battlefield Injuries

PRINCIPAL INVESTIGATOR: David L. Stocum

CONTRACTING ORGANIZATION: Indiana University
Indianapolis, IN 46202

REPORT DATE: October 2014

TYPE OF REPORT: Annual

PREPARED FOR: U.S. Army Medical Research and Materiel Command
Fort Detrick, Maryland 21702-5012

DISTRIBUTION STATEMENT: Approved for Public Release;
Distribution Unlimited

The views, opinions and/or findings contained in this report are those of the author(s) and should not be construed as an official Department of the Army position, policy or decision unless so designated by other documentation.

REPORT DOCUMENTATION PAGE

Form Approved
OMB No. 0704-0188

1. REPORT DATE	2. REPORT TYPE	3. DATES COVERED
October 2014	Annual	19 Sep 2013 - 18 Sep 2014

4. TITLE AND SUBTITLE

Regenerative Medicine for Battlefield Injuries

5a. CONTRACT NUMBER

5b. GRANT NUMBER
W81XWH-11-1-0743

5c. PROGRAM ELEMENT NUMBER

6. AUTHOR(S)

David L. Stocum

E-Mail: dstocum@iupui.edu

5d. PROJECT NUMBER

5e. TASK NUMBER

5f. WORK UNIT NUMBER

7. PERFORMING ORGANIZATION NAME(S) AND ADDRESS(ES)
Indiana University
Indianapolis, IN 46202

8. PERFORMING ORGANIZATION REPORT NUMBER

9. SPONSORING / MONITORING AGENCY NAME(S) AND ADDRESS(ES)
U.S. Army Medical Research and Materiel Command
Fort Detrick, Maryland 21702-5012

10. SPONSOR/MONITOR'S ACRONYM(S)

11. SPONSOR/MONITOR'S REPORT NUMBER(S)

12. DISTRIBUTION / AVAILABILITY STATEMENT
Approved for Public Release; Distribution Unlimited

13. SUPPLEMENTARY NOTES

14. ABSTRACT ABSTRACT

The purpose of this research is to identify the optimum combination of growth factors that stimulate cartilage regeneration across a critical size defect (CSD) in the fibula, using the axolotl Ambystoma mexicanum as a model system. The scope of the research is to (1) characterize the ability to regenerate after fracture and across defects of 10%, 20%, 40% and 50% in the absence of intervention; and (2) test combinations of growth factors, blastema protein extract and intact tissue protein extract for their ability to stimulate cartilage regeneration across 50% defects when delivered by an 8-braid pig small intestinal submucosa scaffold (SIS). Fractures, 10% and 20% defects are bridged with regenerated cartilage and bone within three months post-operation in the absence of any further treatment. In year 3, we determined that the growth factor combination of BMP-4 and HGF delivered by 8-braid SIS successfully stimulates regeneration across defects of 50% by three months post-implantation, whereas scaffold alone (controls) fails to do so. We also tested blastema protein extract vs. unamputated limb tissue protein extract, and we tested a tubular SIS scaffold for its ability to promote regeneration across a 40% defect. To our surprise, the blastema protein extract did not promote regeneration, but the unamputated limb protein extract did so as well as the BMP-4/HGF combination. We also found that grafting axolotl cartilage and muscle to long bone defects in Xenopus hindlimbs were able to promote regeneration, suggesting that cartilage and muscle contain the factors necessary for regeneration. Also to our surprise, the tubular SIS delivery scaffold failed to promote regeneration. We showed that this failure is not due to dissimilar release kinetics (at least of BMP-4) compared to the 8-braid scaffold. Our results have established limb bones of the axolotl as an excellent system to study ways by which to stimulate regeneration across segment defects equal or greater to critical size. A manuscript draft of our results has been prepared and is being modified for publication.

15. SUBJECT TERMS Axolotl hindlimb model, fibula, temporal characterization of fracture repair, characterization of repair of 10-50% segment defects, determination of critical size defect (CSD), SIS scaffold, protein release kinetics.

16. SECURITY CLASSIFICATION OF:			17. LIMITATION OF ABSTRACT	18. NUMBER OF PAGES	19a. NAME OF RESPONSIBLE PERSON
a. REPORT	b. ABSTRACT	c. THIS PAGE			USAMRMC
U	U	U	UU	28	19b. TELEPHONE NUMBER *(include area code)*

Table of Contents

Introduction

The subject of our research is development of the urodele salamander Ambystoma mexicanum (axolotl), as a model to find the optimum set of growth factors that will enable regeneration of a cartilage template across a CSD in the long bones of the extremities across a critical size defect (CSD). Unlike most models that attempt to regenerate bone directly, with less than optimum filling, regeneration of a cartilage template mimics the initial step of both the normal development of a long bone and fracture repair. The axolotl model can be used to screen single molecules or combinations of molecules for their ability to stimulate regeneration across a CSD. This model has advantages over mammalian CSD models in that there is greater ease of surgical operation and tissue processing, no requirement for bone fixation, and is less expensive to maintain. Our purpose is to identify the optimum combination of growth factors that simulate cartilage regeneration across a CSD (and ultimately, the optimum scaffold to deliver these factors). The scope of our research includes the anatomical and histological characterization of cartilage and bone regeneration after fracture and creating defects of 10%, 20%, 40% and 50% segment defects less in the fibula, and identifying optimum combinations of factors that will promote regeneration across 50% defects when delivered from an 8-braid SIS scaffold.

Body

We report here the research accomplishments during the third year period from October 16, 2013 to October 16, 2014. The objectives to be achieved were to: (1) analyze the results of the BMP-4/HGF growth factor combination on regeneration across 50% defects; (2) analyze the results of blastema and unamputated limb tissue protein extract on regeneration across 50% defects; (3) test a tubular SIS scaffold as a delivery vehicle for BMP-4/HGF and protein extract in promoting regeneration across a 40% defect; (4) characterize the release kinetics of BMP-4 from 8-braid and tubular SIS scaffolds; (5) produce a draft of our results to be used for publication.

1. Tests of BMP-4/HGF (Figures 9-11, Table 4, Appendix)

Control defects implanted with scaffold alone did not exhibit any regeneration at three months post-operation. Significant regeneration across 50% defects was obtained with SIS braid soaked in BMP-4/HGF, as shown by the methylene blue stained specimens in Figs. 1-4. In many cases, the segment defect was more on the order of 80%, due to regression of the cut ends of the fibula. Nevertheless, complete bridging was accomplished in several cases. None of the other combinations had a significant effect. No greater frequency or degree of regeneration was observed in the BMPP-4/HGF at 5 months, and the cartilage that had regenerated was undergoing or had undergone ossification (Figs. 5-7). None of the other combinations evoked had evoked regeneration at 5 months. We concluded that the BMP-4/HGF and unamputated limb tissue extract are sufficient to evoke significant regeneration, and that a 3 months time frame is sufficient for

skeletal tissue to regenerate across a 50% defect. In addition, our observations suggested that the observed regeneration can take place from either the proximal, distal, or both cut ends of the fibula.

2. Test of blastema protein extract and protein extract of intact limb tissue (Figures 11, 12, Table 4, Appendix)

Blastema protein extract failed to promote regeneration across a 50% defect, whereas protein extract of unamputated limb tissue extract did so. We concluded that unamputated limb tissue extract is as effective as BMP-4/HGF in evoking significant regeneration, and that a 3 months time frame is sufficient for skeletal tissue to regenerate across a 50% defect.

3. Test of a tubular SIS scaffold as a delivery vehicle

In both 40% and 50% defects the remaining ends of the fibula are not stable, often making an angle to one another, so that cartilage regeneration from the ends of the fibula was not aligned with the original longitudinal axis of the bone. To provide this alignment while simultaneously delivering BMP4/HGF or tissue extract, Cook Biotech made us a tubular SIS scaffold. After soaking in BMP4/HGF or tissue extract, the ends of this scaffold were slipped over the cut ends of the fibula, maintaining alignment until the scaffolds degrades, by which time cartilage regeneration will be underway.

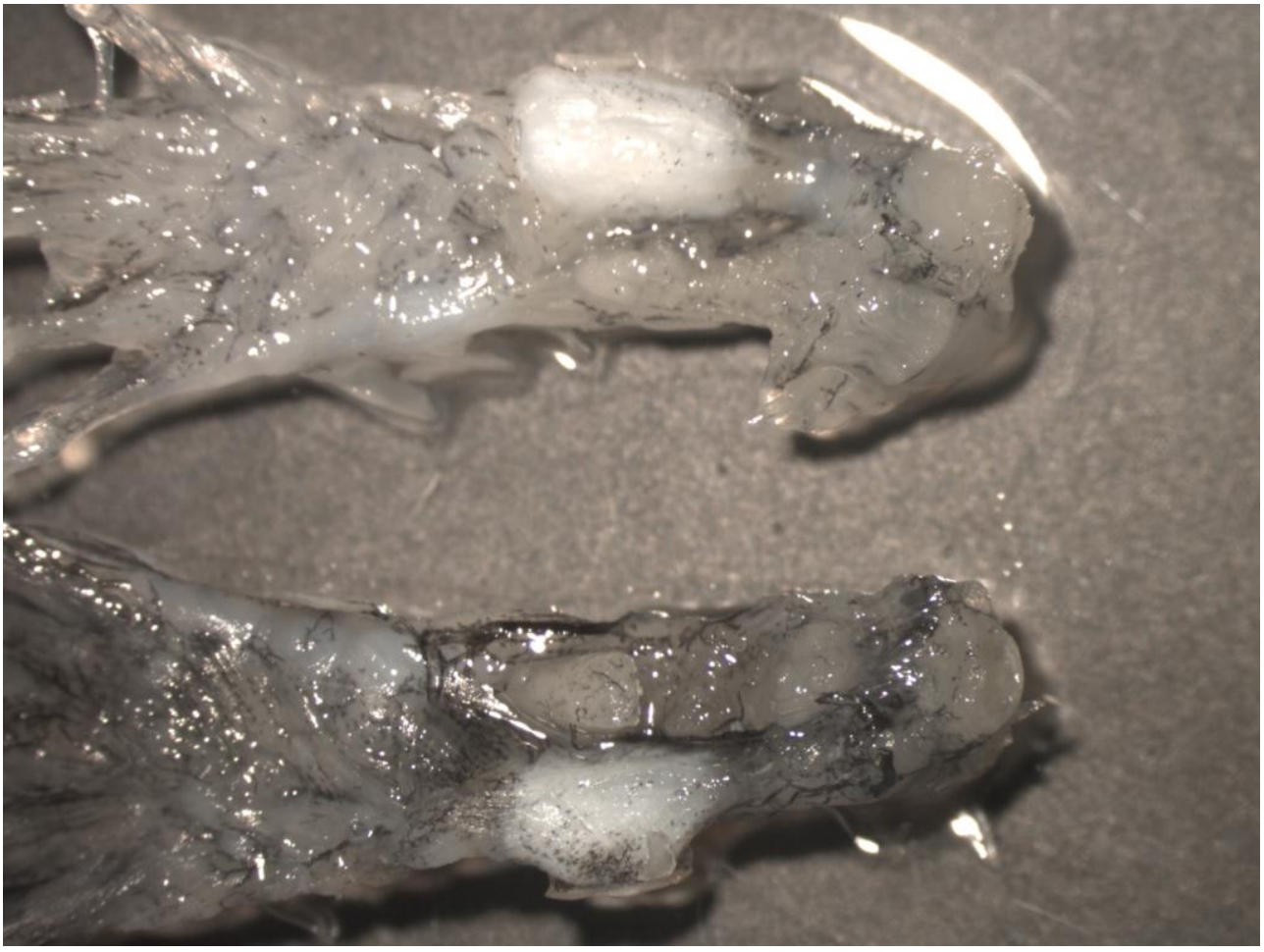

At the same time, we reduced the size of the segment defect to 40%, a gap size that is also not bridged by regenerating skeletal tissue. In the **Figure** above, the SIS tube is white, and has been infiltrated superficially by pigment cells (white dots). Note that the scaffold does not exhibit any breakdown.

A total of 22 experimental limbs were harvested at 3+ months post-implantation. The limbs were distributed among the following treatments:
Scaffolds soaked in tissue extract: 8 limbs
Scaffolds soaked in a combination of BMP4 + HGF: 8 limbs
Scaffolds soaked in BMP4 alone: 3 limbs
Scaffolds soaked in HGF alone: 3 limbs

The scaffold remained in place in these experiments, but contrary to expectation, no regeneration took place within its lumen. We found no skeletal tissue bridging the gap in any of the treatment groups. The explanation for this result does not appear to lie in differential release kinetics of factors from the scaffold, since these do not differ significantly for braid and tubular SIS (see ahead). Growth factors would have been released both toward the outside and inside of the tubular scaffold, and it was our hope that confinement of factors within the tube would lead to enhanced regeneration. Another explanation might be that in order to regenerate cartilage, factors released from the scaffold need to synergize with factors made by surrounding muscle or connective tissue cells. The braid, with its large spaces, would allow this, whereas the walls of the tube may have been too compact to do so. Some evidence that this could be the case was the fact that the tube did not appear to break down as easily as the braid. On the other hand, since factors are released to the outside of the tube, we might expect that cartilage would be induced from periosteal cells of the neighboring tibia. We did not observe such cartilage formation, however. Another possibility to be considered is that swelling of the hydrated scaffold closed off the lumen, becoming a mechanical impediment to regeneration. We are sectioning these specimens to see if there is any sign of lumen closure along with regeneration that was initiated but thwarted. Still another issue to be investigated is the apparent lack of breakdown of the tubular scaffold. Finally, another experimental alternative that should be tested is the use of growth factor-soaked SIS rods along side the defect space rather than in it.

In addition, we performed an experiment in which a length of GFP fibula has been grafted next to (not into!) a 40% segment defect to determine whether cells move laterally into the defect space to make the cartilage template. The result indicates that they do not, and that the regeneration we have documented previously occurs by proliferation from the cut **ends** of the fibula, either from the periosteum, the cartilage, or both.

4. ***Release kinetics of BMP-4 and immunohistochemical staining (Figures 13-16, Appendix)***

We tested the release kinetics of BMP-4 from both braid and tubular SIS scaffolds. Three scaffolds at a time were soaked in 50 μl of BMP-4 solution (10 ng/μl) at 4^{o} C overnight. Each individual scaffold was then serially transferred to new Eppendorf tubes containing 50 μl of 0.8x aPBS and allowed to release for 2 hr., 4hr, 8hr, 1 day, 2 days, and 3 days at room temperature. The concentration of BMP-4 per 50 μl of BMP-4 released into the 50 μl of aPBS at each time point was measured using a human BMP-4 Quantikine ELISA kit (R & D Systems, Minneapolis, MN).

Figure 13 Appendix shows the pattern of release kinetics for BMP-4 from both the 8-braid and tubular SIS scaffolds. Both scaffolds showed an initial burst of BMP-4 release at 2 hr that was 1.25x higher for the braid scaffold. Both scaffolds showed sustained release of BMP-4 at around 100 pg over the next three days. Thus it would appear that a difference in release kinetics of growth factors or tissue extract proteins from the tubular scaffold was not responsible for the lack of regeneration observed with this scaffold.

We also used immunohistochemical staining of BMP-4 and HGF after treatment with BMP-4/HGF or unamputated limb tissue extract. Sample slides were de-waxed in xylene and rehydrated in descending grades of ethyl alcohol. Antigen retrieval was carried out in boiled sodium citrate buffer (10mM Sodium Citrate, 0.05% Tween 20, pH 6.0, Sigma, St. Louis, MO) prior to immunohistochemical staining. Slides were washed briefly in 1x PBS and blocked in 1:50 goat or horse serum (ABC kit, Vector Labs, Burlingame, CA) for 1h at room temperature. Anti-BMP4 (Peprotech, Rocky Hill, NJ) and anti-HGF (Abcam, Cambridge, MA) primary antibodies were applied on samples separately and incubated overnight at 4^{0} C. After washing the slides in 1x PBS, HRP conjugate second antibody was added for 1 h at room temperature. Slides were rinsed in 1x PBS and substrate added for 30 minutes at room temperature (DAB Peroxidase (HRP) substrate kit, Vector Labs, Burlingame, CA). After washing the slides in 1xPBS, ABC reaction solution (Buffalo Grove, IL) was added on the slides and the reaction was detected microscopically at 10x magnification. The anti-BMP4 reaction was stopped after 1.5 minutes and the anti-HGF reaction at 2 minutes in 1x PBS. The slides were then stained in Harris hematoxylin solution for 30 seconds and blued in running tap water, after which they were dehydrated in ascending grades of ethyl alcohol and cleared in xylene. Slides were mounted using Mounting Media & Section Adhesive (Leica Biosystems, Buffalo Grove, IL) and imaged at 40x magnification.

Figures 14-16 Appendix show the results of the staining for cartilage tissue. The BMP4 and HGF signal is strong in chondrocytes after treatment with BMP4/HGF (**Fig. 14)**, BMP4/VEGF (**Fig. 15),** or tissue extract (**Fig. 16).** Similar expression was observed in the muscle and epidermis (not shown).

5. Manuscript draft

We had originally intended to first publish the results of control experiments describing the regeneration of 10%, 20%, 49% and 50% fibular defects, followed by a second paper describing the results of the growth factor experiments. We sent the original paper to the journal Bone, but it was rejected because the reviewers felt that the growth factor data should be presented as well. I agree with this assessment, and we have now put all of our results into one manuscript, a draft of which is provided in the **Appendix.**

Key Research Accomplishments

- Established that BMP-4/HGF and protein extract of whole, unamputated limb tissue can promote regeneration across a 50% segment defect in the fibula, whereas other growth factor combinations either promote only a minimal response or no response.
- A tubular SIS scaffold failed to support regeneration across a 40% segment defect, for unknown reasons.
- Release kinetics profiles were obtained for BMP-4 release from 8-braid and tubular SIS scaffold. There was no significant difference between the profiles.
- A manuscript draft for publication was assembled.

Conclusion

BMP-4/HGF and whole unamputated limb tissue protein extract delivered from an 8-braid SIS scaffold both promote cartilage and bone regeneration across 50% defects in the axolotl fibula. By contrast, use of a tubular SIS scaffold to deliver the same regenerative factors to a 40% defect failed to promote regeneration. This difference does not appear due to differences in the release kinetics profile of BMP-4 between the two scaffolds. We can conclude that the axolotl is a new and suitable model for the study of regeneration across segment defects that has several advantages over other models including cost and ease of *in vivo* screening of regenerating-promoting molecules and scaffolds.

Supporting Data

Table 1: Growth factors implicated by bioinformatic analysis in cartilage and bone regeneration, and in fracture repair.

Growth Factor	Fracture Repair	Cartilage Regeneration	Bone Regeneration
FGF-2	+	+	+
PDGF-A	+	+	+
HGF	+	+	+
TGF-β 1, 2	+	+	+
TGF-β3	+	+	+
Lefty-2	+	+	+
EGF	+	-	+
PDGF B	+	-	+
PDGF D	+	-	+
VEGF A	-	+	+
Follistatin	+	-	-

Table 2: Growth factor combinations and concentrations used to induce cartilage regeneration across 50% defects in the axolotl fibula.

Treatment Group	GF Concentration	# of limbs
1. Amphibian PBS	---	10
2. BMP-4	10 ng/µl	10
VEGF	25 ng/µl	
3. BMP-4	10 ng/µl	10
HGF	10 ng/µl	
4. BMP-4	10 ng/µl	10
VEGF	25 ng/µl	
HGF	10 ng/µl	
5. BMP-4	10 ng/µl	10
VEGF	25 ng/µl	
HGF	10 ng/µl	
FGF-2	8 ng/µl	
6. BMP-4	10 ng/µl	10
VEGF	25 ng/µl	
HGF	25 ng/µl	
FGF-2	8 ng/µl	
EGF	10 ng/µl	
TGFβ-3	2ng/µl	
PDGF-AA	10 ng/µl	
7. Blastema protein extract	7µg/µl	10
8. Limb protein extract	6µg/µl	10

Table 3: Regeneration of cartilage in the absence of intervention across defects of 10%, 20%, 40% and 50% in the axolotl fibula. Fracture data is two months post-operation; 10%, 20%, 40% and 50% data is three months post-operation.

Defect Type	**Regeneration (# of Limbs)**
Fracture	12/12
10%	8/10
20%	7/8
40%	0/8
50%	0/10

Table 4: Number of limbs in which growth factors and limb tissue extract induced partial or significant/complete regeneration across 50% defects in the axolotl fibula at three months post-operation. Partial regeneration means that a small amount of cartilage/bone regenerated from one or both cut ends of the fibula. Significant regeneration means that skeletal regeneration spanned more than 50% of the defect.

	Partial Regeneration	**Significant Regeneration**
Seven Factors	1/12	0/12
BMP-4/VEGF	2/12	0/12
BMP-4/HGF	1/12	4/12
Limb Tissue Extract	2/12	4/12

Appendix

Manuscript titled “Induction of Regeneration Across a Greater Than Critical Size Defect in the Aolotl Fibula”

Induction of Regeneration Across a Greater Than Critical Size Defect in the Axolotl Fibula

By

Xiaoping Chen[1], Fengyu Song[2], Jiliang Li[1], Deepali Jhamb[3], Sahar Alshalchi[1] Ellen Hicks[1], Marco Bottino[2], Mathew Palakal[3] and David L. Stocum[1]*

[1]Department of Biology and Center for Developmental and Regenerative Biology
Indiana University-Purdue University Indianapolis
723 W. Michigan St.
Indianapolis, IN, 46202 USA

[2]Department of Oral Biology and Center for Developmental and Regenerative Biology
School of Dentistry
Indiana-University-Purdue University Indianapolis
1121 W. Michigan St.
Indianapolis, IN 46202 USA

[3]School of Informatics and Computing
Indiana University-Purdue University Indianapolis
Indianapolis, IN 46202 USA

***Corresponding author**

Research supported by grant W81XWH-11-1-0743from the Telemedicine & Advanced Technology Research Center (TATRC), United States Army Medical Research and Materiel Command (USAMRMMC).

Introduction

Mammalian bones fail to regenerate across gaps that exceed the critical size defect (CSD), defined as the smallest defect size that cannot be bridged by regenerated skeletal tissue over the life of the animal [Spicer et al, 2012]. CSDs in human patients are most often caused by the surgical necessity of removing a bone segment damaged by trauma or disease [Harris et al, 2013]. For example, penetrating and blast injuries are particularly damaging to the extremities, creating a challenge for repairing a CSD to avoid amputation [Masini et al, 2009]. Several methods are used to repair CSDs, including bone grafts and prosthetics, but the functional result is often unsatisfactory. Bone autografts, while immunologically acceptable, are not ideal because of a limited number of donor sites and potential morbidity of the donor site. Processed (decellularized) bone allografts circumvent this limitation, but are prone to complications such as infection, non-union, and stress fracture [Garbuz et al, 1988; Stevenson, 1999].

Orthopedic regenerative medicine seeks new strategies aimed at improving regeneration across CSDs of both intramembranous and endochondral bones. These strategies include the use of osteoinductive and osteoconductive scaffolds, with or without osteogenic cells and/or growth factors or growth factor genes, to promote regeneration [Cancedda et al, 2007; Patterson et al. 2008; Nguyen et al, 2012; Cameron et al, 2013; Fisher and Mauck, 2013, Harris et al, 2013, for reviews]. While partly successful, none of these strategies has attained clinical status, due to less than optimal bone regeneration and/or integration with the remaining bone ends. Suboptimal bone regeneration in CSDs of endochondral long bones may be due in part to a focus on direct bone regeneration, rather than on reproducing the actual process of endochondral bone development and fracture repair, which is to first develop a cartilage template that is replaced by bone [Cameron et al, 2013; Li and Stocum, 2014]. Since hypertrophied cartilage itself releases factors that induce osteogenesis [Kanczler and Oreffo, 2008], inducing the regeneration of cartilage in CSDs should be sufficient to lead to bone formation.

The vast majority of studies on segment defects in endochondral bones have been carried out on mice, rats, rabbits and sheep. Amphibians represent a new model for the study of segment defect regeneration in long bones of the extremities [Song et al, 2010; Cameron et al, 2013]. Compared to mammals, amphibians have the advantage of ease and low cost of maintenance, rapid wound healing, no requirement for bone fixation, ease of post-operative care, and low morbidity and mortality. Little, however, has been done to exploit amphibian models for orthopedic research except for the work of Feng et al [2011] on defects in the tarsal bone of *Xenopus laevis* (see Discussion).

The urodele salamander *Ambystoma mexicanum* (axolotl) is another amphibian with unique potential for the study of segment defect regeneration in long bones. The axolotl is native to canals that are the remnant of Lake Xochimilco in Mexico City. It is a neotenous salamander, meaning that it becomes sexually mature in the larval form and does not metamorphose, spending its whole life in the water and retaining gills for respiration (**Fig. 1)**. Axolotls and other urodele salamanders and newts have

immense powers of regeneration, being able to replace amputated limbs, tails, jaws, ventricular tip of the heart, and spinal cord [Stocum, 2012, for review]. In spite of their ability to regenerate amputated limbs, axolotls –like *Xenopus* and mammals—are unable to regenerate across large defects in long bones [Hutchison et al, 2007; Satoh et al, 2010].

As a first step in development of the axolotl as a model to investigate the basic biology and efficacy of different combinations of soluble factors, gene constructs and natural and synthetic scaffolds as regenerative therapies for CSDs of long bones, we report here the results of experiments on segment defects in the fibula of young adult axolotls. We found that the axolotl fibula can repair fractures and regenerate across defects of 10% and 20% of its length in the absence of any therapeutic intervention, but cannot regenerate across defects of 40% or 50%. In a screen for growth factor combinations and protein extracts that would promote regeneration across 50% defects, we found that a combination of BMP-4 and HGF, as well as limb tissue protein extract could stimulate skeletal regeneration when delivered by a pig small intestine submucosa (SIS) scaffold.

Materials and Methods

In Silico Identification of Growth Factors Involved in Fracture Repair

Multiple bone morphogenetic proteins (BMPs) have been implicated in skeletal development and regeneration [Gilbert, 2010]. We have previously used bait proteins and bioinformatics techniques to mine the literature and construct pathways and networks of protein interactions that operate during blastema formation in amputated axolotl limbs (Rao et al, 2009; Jhamb et al, 2011). Here we used the same techniques to mine the literature on fracture repair, cartilage regeneration, and bone regeneration to identify growth factors in addition to BMPs that might be used to stimulate regeneration across segment defects. Keywords related to the process of cartilage differentiation were identified and submitted to the in-house literature-mining tool BioMAP. BioMAP uses a multi-level approach to identify these entities: (1) Part-of speech (POS) tagging by Brill Tagger to identify the noun phrases from the text. (2) Biological entity classification (such as genes, proteins, cell type, organism etc.) for the noun phrases by using the UMLS and other dictionaries such as LocusLink and (3) Hidden Markov Models and N-gram, machine-learning methods, to identify biological entities not discovered by dictionary matching.

The information extracted by BioMAP was normalized using the protein and gene names from the UniProt database. The Human Protein Reference Database (HPRD) was then used to identify growth factors and transcription factors from this gene/protein list. These growth factors and transcription factors were used to determine the predominant pathways and networks of protein interaction in cartilage regeneration (Jhamb et al, unpublished results), using MetaCore^{TM} (GeneGO Inc). These were further analyzed using four topological parameters of the CytoHubba plugin in Cytoscape to select the proteins most commonly identified as significant. The topological properties evaluated were: bottleneck nodes, maximal cliques (MCC), eccentricity, and maximum connected component (MNC).

Eleven growth factors emerged from this analysis: FGF-2, PDGF-A, PDGF-B, PDGF-D, EGF, HGF, TGF-β2, TGF-β3, Follistatin, VEGF-A, and Lefty-2. Nine of these factors have been implicated experimentally in fracture repair, nine in bone

regeneration, and seven in cartilage regeneration (**Table 1**). TGF-β2 and FGF-2 have been implicated in soft callus chondrogenesis, and HGF and PDGF-BB accelerate fracture repair [Nikolaou and Tsiridis, 2007]. HGF does this by facilitating the expression of BMP receptors [Imai et al, 2005]. Lefty-2, which is involved in left/right asymmetry during embryogenesis [Tabin, 2006, for review], has not been implicated experimentally in skeletal development and regeneration.

Seven of these growth factors, in addition to BMPs, were commercially available: VEGF-A, HGF, FGF-2, TGF-β3, PDGF-AA, PDGF-BB, and EGF. All of these, except EGF and PDGF-BB, had an amino acid sequence homology to the corresponding *Xenopus* growth factors (the closest amphibian to the axolotl for which such data were available) of 64% or greater. EGF and PDGF-BB were eliminated from consideration because of their low homologies (41% and 39%, respectively). Six different combinations of BMP-4 and the remaining five growth factors were tested for their ability to promote regeneration across a 50% segment defect, which exceeds the CSD (**Table 2**). The concentrations chosen for the growth factors were estimated from published reports in which single growth factors were used to promote regeneration across segment defects [Lepisto et al, 1992; Shah et al, 1996; Opperman et al, 2000; Seeherman et al, 2002; Yun et al, 2010). All growth factors were purchased from PeproTech (Rocky Hill, NJ) and stock solutions of each prepared according to instructions provided by the company. These were used to prepare the combinatorial solutions, which were diluted to the final treatment concentration with filtered 0.8X aPBS.

We also tested the ability of protein extract from axolotl medium bud regeneration blastema and from intact whole limb tissue to promote regeneration (**Table 2**). Tissues were ground in liquid nitrogen and cell lysis buffer in the presence of proteinase inhibitors (RayBio). Bradford assay indicated that the protein concentration of the extracts was approximately 5.76 mg/ml. These extracts induced no inflammatory reaction when injected into the muscle of the hindlimb.

Animals and Surgery: Axolotl larvae from the Ambystoma Stock Center at the University of Kentucky (Lexington) were raised to a length of 12-15 cm (nose to tail tip, young adults). They were maintained in individual containers with daily changes of artificial pond water (10% Holtfreter solution) and fed salmon chow daily (Rangen, Buhl, Idaho). Axolotls (unfed for 24 hrs prior to surgery) were anesthetized by immersion in 0.1% (w/v) of MS-222 (Fisher Scientific, Pittsburgh PA) in 10% Holtfreter solution buffered with bicarbonate to pH 7.3. A simple cut with microscissors through the mid-diaphysis was used to create a fracture of the fibula. To create a segment defect, the length of the fibula was first measured externally with calipers. A cut was made with microscissors in the posterior skin of the hind limb and the muscle pushed to one side to expose the fibula. A length of bone equivalent to a defect of 10%, 20%, 40% or 50% of the total fibula length was then excised from the middle of the bone. The average length of the fibula was 7 mm. The average length of the defects was thus 0.7 mm, 1.4 mm, 2.8 mm, and 3.5 mm, respectively. The animals were kept immersed in 0.01% MS-222 to control pain during a recovery period of two hours, and then returned to artificial pond water. The wounds healed within one week without other treatment.

Defects of 50% were used to test growth factor combinations. Growth factor or tissue extract-loaded scaffolds were inserted into 50% defects and the wound was closed with two sutures of #6 silk thread (Fine Science Tools, Inc., Foster City, CA). Controls consisted of limbs in which the fibular defect received no treatment or was implanted with scaffold soaked overnight at 4^{o} C in 0.8x aPBS.

Loading of SIS Scaffold with Growth Factors or Tissue Extracts

An eight-strand biodegradable braid of SIS, a generous gift from Cook Biotech (West Lafayette, IN), was used to deliver combinations of growth factors and tissue extracts to 50% segment defects. The braid was half the diameter of the fibula and hydrated to the diameter of the fibula when soaked in growth factor solution prior to implantation into a segment defect. The braid was cut into pieces approximating the length of the segment defect that were then sterilized for 30 min with UV light. For a given experiment, five sterile pieces were immersed overnight at 4^{o}C in 50 μl of sterile growth factor or tissue extract solution contained in the inverted cap of a 1 ml Eppendorf tube. The cap in turn was placed in a small culture dish floored with sterile moist paper to maintain humidity and prevent changes in concentration of the solutions.

Release Kinetics of BMP-4 from SIS Scaffold

Kinetics of protein release was analyzed for BMP-4. Three scaffolds at a time were soaked in 50 μl of BMP-4 solution (10 ng/μl) at 4^{o} C overnight. Each individual scaffold was then serially transferred to new Eppendorf tubes containing 50 μl of 0.8x aPBS and allowed to release for 2 hr., 4hr, 8hr, 1 day, 2 days, and 3 days at room temperature. The concentration of BMP-4 per 50 μl of BMP-4 released into the 50 μl of aPBS at each time point was measured using a human BMP-4 Quantikine ELISA kit (R & D Systems, Minneapolis, MN).

3. Immunohistochemistry staining

Sample slides were de-waxed in xylene and rehydrated in descending grades of ethyl alcohol. Antigen retrieval was carried out in boiled sodium citrate buffer (10mM Sodium Citrate, 0.05% Tween 20, pH 6.0, Sigma, St. Louis, MO) prior to immunohistochemical staining. Slides were washed briefly in 1x PBS and blocked in 1:50 goat or horse serum (ABC kit, Vector Labs, Burlingame, CA) for 1h at room temperature. Anti-BMP4 (Peprotech, Rocky Hill, NJ) and anti-HGF (Abcam, Cambridge, MA) primary antibodies were applied on samples separately and incubated overnight at 4^{0} C. After washing the slides in 1x PBS, HRP conjugate second antibody was added for 1 h at room temperature. Slides were rinsed in 1x PBS and substrate added for 30 minutes at room temperature (DAB Peroxidase (HRP) substrate kit, Vector Labs, Burlingame, CA). After washing the slides in 1xPBS, ABC reaction solution (Buffalo Grove, IL) was added on the slides and the reaction was detected microscopically at 10x

magnification. The anti-BMP4 reaction was stopped after 1.5 minutes and the anti-HGF reaction at 2 minutes in 1x PBS. The slides were then stained in Harris hematoxylin solution for 30 seconds and blued in running tap water, after which they were dehydrated in ascending grades of ethyl alcohol and cleared in xylene. Slides were mounted using Mounting Media & Section Adhesive (Leica Biosystems, Buffalo Grove, IL) and imaged at 40x magnification.

Imaging

All limbs were harvested at intervals of two to three months, and fixed for one week in 10% buffered formalin.

X-Ray and computed tomography: All of the fixed limbs for each time point were first imaged by X-ray (PIXARRAY 100, Bioptics, San Jose, Costa Rica) and then by microcomputed tomography (micro-CT), using a high-resolution desktop imaging system (SkyScan 1172, Allentown, PA). The micro-CT scans included the region from the distal end of the femur to the proximal tarsus and were obtained using an X-ray source set at 60kV and 167 μA over a angular range of 180 ^{o} (rotational steps of 0.9^{o}) with a 17-μm pixel size. NRecon Reconstruction software was used to construct cross-sectional images with up to 8000 x 8000 pixels, which were then used to reconstruct a volumetric 3-D image. These techniques image ossified tissue, but do not image cartilage formation. Bone volume per total volume (BV/TV) was calculated at the defective region in each animal.

Whole mounts and histology: Half of the samples for each time point were stained in 0.25% methylene blue for cartilage matrix, or double-stained in methylene blue and alizarin red for both cartilage and bone matrix. The other half of the fixed specimens was decalcified in Calciclear (Fisher Scientific, Pittsburgh, PA) for three weeks at room temperature, embedded in paraffin (Fisher Scientific), sectioned at 10 μm, and stained with Ehrlich's hematoxylin and eosin (Fisher Scientific). Some slides were stained with Gomori's Trichrome stain (Polysciences, Warrington, PA) after being re-fixed overnight in Bouin's solution after the re-hydration step. Imaging was done on a Leica model DM2000 light microscope equipped with a camera (Leica Microsystems, Buffalo Grove, IL).

Fluorochrome Imaging: Two fluorochromes were used to measure early bone regeneration in untreated 10% vs. 50% defects. On the day of surgery, a 1% calcein solution (Sigma Chemical, St. Louis, MO) was injected subcutaneously into the proximal one-third of the hind limb zeugopodium at a dose of 15μg/gm body wt. This fluorochrome fluoresces green. One week after the surgery, a solution of 3% alizarin complexone red was injected at the same site at a dose of 30 μg/gm body wt. This fluorochrome fluoresces red. The limbs were harvested at 3 weeks post-surgery and fixed in 10% neutral formalin solution for one week. The soft tissues were removed with jeweler's forceps and the fibular bone on either side of the defect was imaged whole with Leica fluorescent optics for red and green fluorescence (Leica Microsystems, Buffalo Grove, IL). Two color images

were merged using Image J software and the extent of bone regeneration was assessed by measuring the length of red color extending from green color on the anterior, middle and posterior sides of the bone.

Results

Controls: Untreated Defects and Defects Implanted With Scaffold Alone

Table 3 summarizes the results of regeneration in the absence of any treatment or after implanting 8-braid scaffold alone. One hundred percent of untreated fractures and 80-88% of the 10% and 20% segment defects repaired the defect with regenerated cartilage by two months post-operation. Faint shadows indicative of bone regeneration were observed two months post-operation by X-ray imaging in the 10% and 20% defects, and micro-CT scans confirmed that ossifcation had taken place (**Fig. 2**). **Figure 3** illustrates examples of methylene blue/alizarin red staining of whole mounts and H&E-stained sections of regenerated tissue at 3 months post-operation. The new bone formed an irregular bridge connecting the cut ends of the fibula.

The process of regeneration appeared to be very similar in fractures and 10% segment defects, which were bridged within 2-3 weeks with cartilage that ossified earlier than in 20% defects. Examination of sections at three weeks post-operation indicated that in the 20% defects, the ossification centers arose not in the center of the cartilage bridge, as in the development of endochondral bones, but in the cartilage regenerating from each end of the fibula, suggesting that regeneration took place from both ends of the cut bone toward the center. Flattened chondrocytes, hypertrophying chondrocytes, and regions of osteogenesis with osteoblasts and osteoclasts were observed extending from the ends of the bone in these sections.

None of the untreated 40% and 50% defects showed any regeneration by three months post-operation. X-ray and CT scans were negative at all time points. Methylene blue/alizarin red whole mount staining and sections stained with H&E showed clearly that no skeletal tissue had regenerated across the defects at three months post-operation and that the defects were instead filled with disorganized fibrous connective tissue and regenerated muscle **(Fig. 4)**. In all cases, the cut ends of the fibula were simply capped off and the defects were filled in with fibrous connective tissue and muscle. Additional experiments showed that 40% and 50% defects did not exhibit regeneration of skeletal tissue even after 6 months. If the CSD is defined as the smallest size defect that will not regenerate over the course of our experiments, these data indicate that the CSD for the axolotl fibula is between 20% and 40%.

Figure 5 shows the newly regenerated bone volume fraction (BVF). In the 10% defects, the BVF was 74.4% and in the 20% defects it was 70.6%. The BVF for the 40% defects was 38.7%, and for the 50% defects, 11.3%. We used calcium-binding fluorochromes (Pautke et al, 2005) to visualize sites of active mineralization in 10% vs. 50% defects in the fibula. In merged images of calcien (green) and alizarin complexone (red), regeneration of bone is clearly underway in the 10% defect by 3 weeks

post-operation, as indicated by the separation of the green and red colors, whereas virtually no color separation had taken place at the bone ends of the 50% gap (**Fig. 6)**.

To determine whether the 8-braid SIS scaffold would by itself promote regeneration across 40% and 50% defects, we implanted four scaffolds into 40% defects and 16 scaffolds into 50% defects. The braid was hydrated by dipping it into the growth factor carrier, sterile 0.8x aPBS prior to insertion into the defect. Trichrome and H&E staining of sections was used to monitor degradation of the scaffold and the tissue filling the defect space. After three months the defects were filled with disorganized connective tissue and regenerated muscle, but no skeletal tissue had regenerated (**Fig. 7**). These results demonstrate that the SIS scaffold by was unable by itself to stimulate regeneration.

Effect of Growth Factors and Tissue Extracts on 50% Defects

Table 4 shows the results of implanting 50% defects with 8-braid SIS soaked in growth factor or tissue extract solutions. Fifty percent defects were chosen in order to provide a regenerative challenge well beyond the CSD. We noted that in many cases, the bone at the cut ends of the fibula had undergone substantial regression, making the segment defect closer to 70%.

The extent of regeneration fell into two categories, partial and significant. Partial regeneration was defined as bridging less than 25% of the defect, whereas significant regeneration was defined as bridging 50% or more of the defect. The 7-factor combination yielded one case of partial regeneration out of 24 limbs, and the BMP-4/VEGF combination yielded two cases out of 24 limbs. The regenerated skeletal tissue consisted of irregular tongues of cartilage, as illustrated in **Fig. 8A** and **8B.** No cases of significant regeneration resulted from these combinations.The BMP-4/HGF combination yielded one case of partial regeneration and four cases of significant regeneration out of 24 limbs. The case of partial regeneration is illustrated in **Fig. 9.**

BMP4/HGF induced significant regeneration in four out of 24 limbs by two-three months post-implantation. **Figure 10A** illustrates one case where new cartilage surrounded by a shell of bone regenerated the length of the gap, but in parallel with, and adjacent to, the tibia. The origin of the cells of this cartilage was likely the periosteum of the tibia. **Figure 10B** shows a case where regeneration took place over nearly the whole defect from the proximal end of the fibula.

Whole limb tissue extract also was effective at inducing regeneration. Of 24 cases, two had partial regeneration and four had significant regeneration. **Figure 11** shows a specimen in which new cartilage was regenerated under the skin over nearly the complete length of the defect. The origin of the chondrocytes in this case may have been dermal fibroblasts. **Figure 12A, B** illustrates two other cases treated with tissue extract. In **Fig. 12A**, an irregular mass of cartilage has filled the defect and is joined to the tibia by a bridge of cartilage. **Fig. 12B** shows complete regeneration at an angle between misaligned free bone ends to form a shallow V.

None of the other growth factor combinations, or blastema protein extract, evoked any regeneration by three months.

Alternative SIS Scaffold

Our 50% segment defect, made larger by regression of bone tissue at the cut ends of the fibula, far exceeded the CSD. Furthermore, any angling of the free bone ends with respect to the longitudinal axis of the fibula posed an even greater challenge to bridging the defect. To investigate the effect of a smaller defect greater than critical size and a scaffold designed to maintain the alignment of the ends of the fibula in the original longitudinal axis, we did a series of experiments in which we decreased the segment defect size to 40% and used a tubular SIS soaked in BMP-4/HGF or tissue extract. The tubular scaffold was slipped over the cut ends of the bone to prevent their deviation from the long axis. Inexplicably, neither BMP4/HGF nor intact tissue protein extract stimulated regeneration when absorbed by this scaffold.

BMP-4 Release Kinetics and anti-BMP-4 and HGF Immunohistochemistry

Figure 13 shows the pattern of release kinetics for BMP-4 from both the 8-braid and tubular SIS scaffolds. Both scaffolds showed an initial burst of BMP-4 release at 2 hr that was 1.25x higher for the braid scaffold. Both scaffolds showed sustained release of BMP-4 at around 100 pg over the next three days. Thus it would appear that a difference in release kinetics of growth factors or tissue extract proteins from the tubular scaffold was not responsible for the lack of regeneration observed with this scaffold.

Figures 14-16 show the results of the anti-BMP-4 and anti-HGF staining for cartilage tissue in cases treated with BMP-4/HGF, BMP-4/VEGF, or tissue extract . The BMP4 and HGF signal is strong in chondrocytes after treatment with BMP4/HGF (**Fig. 14)**, BMP4/VEGF (**Fig. 15),** or tissue extract (**Fig. 16).** Similar expression was observed in the muscle and epidermis (not shown).

Discussion

Several studies of segment defect regeneration in amphibian long bones have been conducted previously. Young urodele larvae, but not anuran tadpoles or adult newts, were reported able to regenerate extirpated skeletal elements in unamputated limbs [Goss, 1958]. Removal of the ulna from adult newt (*Notophthalmus viridescens)* forelimbs followed by amputation through the middle of the defect resulted in regeneration of the part of the ulna distal to the amputation plane by the blastema, but the part of the ulna proximal to the amputation plane was not regenerated [Goss, 1956]. Korneluk and Liversage [1984] reported that adult newt fore limbs from which both radius and ulna were removed, regenerated the hand after amputation through the distal end of the defect, but did not regenerate the radius/ulna. They also removed the radius/ulna from adult *Xenopus* fore limbs amputated through the distal forelimb, resulting in the formation of a fibroblastema distally and a large gap containing muscle and connective tissue between the fibroblastema and a proximal cartilage remnant of the radius/ulna. The fibroblastema developed into a small cartilage spike. In about half the cases, regeneration of cartilage rods took place in a proximal direction from the base of this spike, and distally from the radius/ulna cartilage remnant, suggesting an attempt to bridge the skeletal gap. The ability to undergo this type of regeneration appeared to be associated with the presence of the fibroblastema, since it did not occur in the

unamputated limb. The influence of a blastema on segment defect regeneration of endochondral limb bones in urodeles might offer additional clues on how to bridge these defects.

Feng et al [2011] demonstrated a failure to bridge large segment defects made in one of the two tarsal bones of the unamputated adult *Xenopus* hind limb. The CSD of the tarsus was determined to be about 35% of the total bone length. They used a biocompatible 1,6 hexanedioldiacrylate (HDDA) scaffold loaded with BMP-4 and VEGF to induce bridging of the CSD by a cartilage template, which was followed by the beginning of osteogenesis in the mid-region of the cartilage. The scaffold did not act as an osteoinductive substrate, but rather to deliver the growth factors over the whole length of the CSD, and was pushed to one side of the regenerating cartilage. Untreated CSDs formed only fibrous scar tissue. A disadvantage of this model was that the HDDA scaffold was not biodegradable.

Hutchison et al [2007] and Satoh et al [2010] found that neither untreated (control) fibula nor radius regenerated across 25%-54% segment defects (as measured from their published photographs). Their data and ours suggest that the CSD for the fibula of small larvae and young adult axolotls is greater than 20%, but less than 40%, perhaps as low as 25%. A more detailed study on regeneration across segment defects between 20% and 40% will be required to provide a more exact estimate of the CSD.

More than half of our 10% and 20% segment defects showed signs of regeneration on X-ray images two months after operation and 100% of the defects were repaired by three months as judged by X-ray, micro CT, whole mount staining for cartilage and bone, and histological examination of stained tissue sections. Cartilage developed first and was replaced by bone. Regeneration appeared to take place by extension from one or both ends of the cut bone. Extension from one end continued to the other end, whereas extensions from both ends met in the middle to bridge the gap. These extensions were often at first irregular in appearance but eventually became more regular as endochondral ossification replaced the cartilage template. The impression from histological examination was that the cells providing the chondrocytes for regeneration came from the periosteum at the cut ends of the bone. The bone volume in the middle of the newly regenerated bone of the 10% and 20% segment defects was more than 50% of the total regenerated bone volume.

In contrast to the 10-20% segment defects, the cut ends of the fibula in 40% and 50% defects were capped off and no regeneration took place across the gaps. These defects were filled in by regenerated muscle and connective tissue that lacked organization. The regenerated bone volume was very low in the capped off ends of the 40% and 50% segment defects. Fluorochrome staining showed clearly that regeneration of calcified skeletal tissue took place in the 10% defects within three weeks, whereas none was initiated in the 50% defects. We also observed that the cut ends of the bone in 40% and 50% defects often underwent regression

such that the defect space was larger than that created by removing the bone segment. Hutchison et al [2007] and Satoh et al [2010] observed a similar loss of bone after creating large segment defects in the long bones of young axolotl larvae.

Scaffold alone did not induce cartilage regeneration across 50% defects. Histological examination indicated that the scaffold degraded over time while the defect was again filled by disorganized muscle fibers and connective tissue. By contrast, Suckow et al [1999] found that SIS by itself could promote regeneration across a 30-40% segment defect (as measured from their published photographs) in the radius of adult rats. Cartilage was observed as early as three weeks and bone as early as six weeks. By 6 months, 75% of the defect in all the rats was filled with radiopaque tissue. The difference between their results and ours may be that the SIS in their experiments was prepared *de novo* without the extensive processing done to create the version of SIS that we used and thus may have retained significant amounts of growth factors that promoted regeneration.

Satoh et al [2010] found that microbeads loaded with BMP-2 were able to stimulate cartilage regeneration across segment defects of various lengths made in the radius of young (3 cm) axolotl larvae. They speculated that the regenerated cartilage was derived from fibroblasts that differentiated directly into chondrocytes without first dedifferentiating, since fibroblasts proliferated without expressing *Prrx-1*, a transcription factor that plays a role in limb development and fibroblast migration (Martin and Olson, 2000; McKean et al 2003) and which is a marker for the dedifferentiated cells that form the regeneration blastema in an amputated axolotl limb. Blastema cells grafted into a segment defect of the radius also differentiated into cartilage. Furthermore, removing the skin over a defect to create a wound epidermis and deviating a nerve into the CSD, two conditions associated with amputation-induced limb regeneration, resulted in cartilage regeneration by the proliferation of fibroblasts that did express *Prrx-1*. This result suggested that the nerve and wound epidermis provided signals that induced histolysis and dedifferentiation to produce blastema cells, similar to what happens in the amputated limb.

Because the axolotls used in our study were young adults with larger and denser bones than young larvae, we reasoned that growth factors in addition to BMPs might enhance or be required to promote regeneration across 50% and larger defects. However, the only combination that promoted significant regeneration of cartilage and bone across 50% segment defects with any consistency was BMP-4/HGF. Partial regeneration was stimulated in one case of the 7-factor cocktail and two cases of the BMP-4/VEGF combination, but none of the other combinations stimulated regeneration.

There could be multiple explanations for these differential results, such as suboptimal growth factor concentrations and/or concentration ratios. A likely part of the explanation, however, is that as in fracture repair, the expression of different growth factors needs to follow a spatial and temporal cascade initiated by BMPs in order to regenerate across a CSD. The involvement of HGF would be through its ability to induce expression of BMP receptors (Imai et al, 2005). The release kinetics profile shows that

after a peak burst at 2 hr and a subsequent 15% decrease by 4 hr, the amount of BMP-4 released is sustained at a relatively steady level of about 75% of the 2 hr value over three days. We did not test BMP-4 or HGF alone, so the possibility remains that either of these growth factors could by themselves initiate the molecular cascade leading to cartilage regeneration. HGF by itself has been found to have an anti-scarring effect in injured laryngeal folds of rats [Xu et al, 2010] and has long been known to be the principal growth factor that activates satellite cells in muscle regeneration [Tatsumi et al, 1998]. In addition, HGF inhibits BMP-2-induced generation of osteoblasts in multiple myeloma, prompting the continued proliferation of MSCs [Standal et al, 2007] and thus could promote chondroblast proliferation in conjunction with BMP-4.

In BMP-4/HGF-treated 50% defects, as in untreated 10% and 20% defects, the regenerating cartilage appears to grow from either or both cut ends of the fibula, suggesting either a periosteal or chondrogenic origin. Cartilage contributes only a small percentage of the blastema cells that regenerate cartilage in an amputated axolotl limb, most regenerated chondrocytes arising by the transdifferentiation of dermal fibroblasts [Steen, 1968; Muneoka et al, 1985]. In mammals, the cartilage that repairs fractured long bones arises from mesenchymal stem cells (MSCs) in the periosteum and endosteum (McKibben, 1978, for review). Thus periosteal/endosteal MSCs may be the source of the regenerated cartilage in our experiments, but transdifferentiation of dermal or muscle fibroblasts to chondrocytes cannot be ruled out. Labeling studies will be required to trace the actual origin(s) of the regenerating cartilage. The cartilage formation induced by BMP-4/HGF is succeeded by ossification to complete the regenerative process through pathways triggered by factors such as VEGF that are expressed by hypertrophied chondrocytes (Einhorn, 1998, for review).

Protein extract of whole limb tissues was also an effective treatment in regenerating cartilage and bone across 50% gaps in the fibula, whereas protein extract of regeneration blastemas had no effect. This result indicates that limb tissue extract contains factors in addition to BMPs and HGF that initiate the molecular cascade leading to cartilage regeneration and ossification. It would be instructive to carry out a targeted quantitative proteomic analysis of this extract, and fractions thereof, to identify these factors. Why blastema protein extract had no effect is puzzling, since the regeneration blastema would be presumed to have all the factors necessary for cartilage differentiation.

Our use of limb protein extract to stimulate regeneration originated in another experiment in which the distal two-thirds of the fibula and tibia were removed from *Xenopus* hind limbs and a graft of axolotl limb muscle and cartilage was inserted into the resulting space (Chen et al, unpublished results). The limb was then amputated through the distal tarsus. A fibroblastema formed at the amputation surface and gave rise to a symmetrical cartilage spike. The axolotl tissue degenerated as a result of host immune response. A cartilaginous rod of *Xenopus* cells bridged the gap between femur and tarsus, in contrast to controls that received no graft and showed no cartilage regeneration in the gap. These results suggested that axolotl limb tissue proteins were released to induce cartilage regeneration across a major defect in the tibia/fibula of the *Xenopus* limb. Partially purified BMP extract of

ostrich and reindeer bones has been reported to promote ectopic bone regeneration in rats (Ulmanen et al, 2005; Pekkarinen et al, 2006) and lyophilized reindeer bone extract in a collagen carrier induced bone regeneration in an 8 mm gap of the rat femur (Tolli et al, 2011).

The BMP-4 release kinetics profile showed that the 8-braid scaffold gave burst of release at 2 hr that dropped plateaued at a slightly lower level that was maintained for at least three days. Antibody staining to BMP-4 and HGF indicated that BMP-4/HGF or VEGF induces expression of BMP-4 and HGF by chondrocytes and muscle. The reasons why our tubular SIS scaffold failed to promote regeneration are unknown. Differences in the release kinetics of BMP-4 do not appear to be responsible for this result. The tubular scaffold would have released growth factors into the interior of the tube and toward the outside of the tube. In addition to maintaining alignment of the cut ends of the fibula with the original longitudinal axis, we had hoped that the BMP-4/HGF and tissue protein extract confined within the tube would interact longer with the tissue of the bone ends. Similar strategies to compartmentalize bone-inducing factors within a CSD space in mammalian bones have used a PMMA spacer [Viateau et al, 2007; Klaue et al, 2009] or PTFE membranes [El-Fayomi et al, 2003] to induce formation of a vascularized membrane around the space. Another possibility is that, in addition to the BMP-4/HGF released by the scaffold, other factors provided by surrounding connective tissues, muscle, nerve and blood vessels are also required to foster cartilage regeneration. This may be one reason why the 8-braid scaffold worked, and the tubular scaffold did not, because such factors would more easily be able to diffuse into the defect space. In any event, the results with the tubular scaffold add to previous observations that the morphology and physical architecture of the scaffold are important parameters in interventions designed to stimulate regeneration across CSDs [Seeherman et al, 2002].

Conclusion

We have established that the axolotl (and most likely other urodele species) can serve as an inexpensive and surgically amenable model to screen different combinations of factors for their ability to promote regeneration of cartilage and bone across a CSD. The model has established that a combination of BMP-4 and HGF, as well as whole limb issue extract is effective in evoking regeneration across gaps of 50% or greater in the axolotl fibula. This model is also amenable to screening different scaffold types to determine what biomaterials have the optimal osteoconductive and osteoinductive properties and architectures for delivery of cartilage cascade-initiating and sustaining factors that promote cartilage regeneration across defects of critical size or greater in long bones. The model may also be informative about skeletal regeneration under conditions of weightlessness, such as are encountered on long space flights, since skeletal regeneration in axolotls takes place in a buoyant environment that mimics reduced gravity.

References

Cameron JA, Milner DJ, Lee JS, Cheng J, Fang NX, Jasiuk IM (2013) Employing the biology of successful fracture repair to heal critical size bone defects. In: Current Topics in Microbiol & Immunol 367: New Perspectives in Regeneration. Heber-Katz E,Stocum DL, eds. Springer-Verlag, Berlin & Heidelberg, pp 113-132.

Cancedda R, Giannoni P, Mastrogiacomo M (2007) A tissue engineering approach to bone repair in large animal models and in clinical practice. Biomaterials 28:4240-4250.

El-Fayomi A, El-Shahat A, Omara M, Safe I (2003) Healing of bone defects by guided bone regeneration (GBR): an experimental study. Egypt J Plast Reconstr Surg 27:159-166.

Feng L, Milner DJ, Xia C, Nye HLD, Redwood P, Cameron JA, Stocum DL, Fang N, Jasiuk I (2011) Long bone critical size defect repair by regeneration in adult *Xenopus laevis* hindlimbs. Tiss Eng Part A, 17:691-701.

Fisher MB, Mauck RL (2013) Tissue engineering and regenerative medicine: Recent innovations and the transition to translation. Tiss Eng Part B 19:1-13.

Garbuz DS, Masri BA, Czitrom AA (1998) Biology of allografting. Orthop Clin North Am 29:199-204.

Gilbert S (2010) Developmental Biology, 9th ed. Sinauer Associates Inc, Sunderland, MA.

Goss RJ (1958) Skeletal regeneration in amphibians. J Embryol exp Morph 6:638-644.

Goss RJ (1956) The relation of bone to the histogenesis of cartilage in regenerating forelimbs and tails of adult Triturus Viridescens. J Morph 98:8

Hamburger V (1960) A Manual of Experimental Embryology. University of Chicago Press, Chicago.

Harris JS, Bemenderfer TB, Wessel AR, Kacena MA (2013) A review of mouse critical size defect models in weight bearing bones. Bone 55:241-247.

Hutchison C, Mireille P, Roy S. The axolotl limb: a model for bone development, regeneration and fracture healing. Bone 2007;40:45-56.

Imai Y, Terai H, Nomura-Furuwatari, Mizano S, Matsumoto K, Nakamura T, Takaoka K (2005) Hepatocyte growth factor contributes to fracture repair by upregulating the expression of BMP receptors. J Bone Mineral Res 20:1723-1730.

Jhamb D, Rao N, Milner DJ, Song F, Cameron JA, Stocum DL, Palakal MJ (2011) Network based transcription factor analysis of regenerating axolotl limbs. BMC Bioinformatics12:80.

Kanzler JM, Oreffo ROC (2008) Osteogenesis and angiogenesis: The potential for engineering bone. European Vells Maters 15: 100-114.

Klaue K, Knothe U, Anton C, et al, (2009) Bone regeneration in long-bone defects: tissue compartmentalization? In vivo study on bone defects in sheep. Injury 40 S4: S95-S102.

Korneluk RG, Liversage RA (1984) Effects of radius-ulna removal on forelimb regeneration in *Xenopus laevis* froglets. J Embryol exp Morph 82:9-24.

Lepisto J, Laato M, Niinikoski J, Lundberg C, Gerdin B, Heldin C-H (Effects of homodimeric isoforms of platelet-derived growth factor (PDGF-AA and PDGF-BB) on wound healing in rat. J Surg Res 53:596-601.

Li J, Stocum DL (2014) Fracture healing. In: Basic and Applied Bone Biology: Burr DB, Allen MR, eds. Elsevier/Academic Press, San Diego, pp 205-224.

Martin JF, Olson EN (2000) Identification of a *Prx1* limb enhancer. Genesis 26:225-229.

Masini B D, Waterman SM, Wenke JC, Owens BD, Hsu JR, Ficke JR (2009) J Orthoped Trauma 23:261-266.

McKean DM, Sisbarro L, Ilic D, Kaplan-Alburquerque N, Nemeroff R, Welser-Evans M, Kern MJ, Jones PL (2003) FAK induces expression of Prx1 to promote tenascin-C-dependent fibroblast migration. J Cell Biol 161:393-402.

Nguyen LH, Annabi N, Nikkah M, Bae H, Park S, Kang Y, Yang Y, Khademhosseini A (2012) Vasclarized bone tissue engineering: Approaches for potential improvement. Tiss Eng Part B: Reviews 18:363-382.

Nikolaou VS, Tsiridis E (2007) Minisymposium: fracture healing (I) Pathways and signaling molecules. Curr Orthopaed 21:249-257.

Opperman LA, Adab K, Gakunga PT (2000) Transforming growth factor-β2 and TGF-β3 regulate fetal rat cranial suture morphogenesis by regulating rates of cell proliferation and apoptosis. Dev Dynam 219:237-247.

Patterson TE, Kumagal K, Griffith L, Muschler GF (2008) Cellular strategies for enhancement of fracture repair. J Bone Joint Surg 90, (Suppl 1):111-119.

Pautke C, Vogt S, Tischer T, Wexel G, Deppe H, Milz S, Schieker, M, Kolk S (2005) Polychrome labeling of bone with seven different fluorochromes: enhancing fluorochrome discrimination by spectral image analysis. Bone 37:441 – 445.

Pekarinen T, Jamsa T, Maatta M, Hietala O, Jalovaara P (2006) Reindeer BMP extract in the healing of critical-size bone defects in the radius of the rabbit. Acta Orthop 77:952-959.

Satoh A, Cummings GMC, Bryant SV, Gardiner DM (2010) Neurotrophic regulation of fibroblast dedifferentiation during limb skeletal regeneration in the axolotl (*Ambystoma mexicanum*). Dev Biol 337:444-457.

Seeherman H, Wozney J, Li R (2002) Bone morphogenetic protein delivery systems. Spine 27 (16S) Supplement:S16-S23.

Shah M, Foreman DM, Ferguson MWJ (1995) Neutralisation of TGF-β1 and TGF-β2 or exogenous addition of TGF-β3 to cutaneous rat wounds reduces scarring. J Cell Sci 108:985-1002.

Song F, Li B, Stocum DL (2010) Amphibians as research models for regenerative medicine. Organogenesis 6:141-150.

Spicer PP, Kretlow JD, Young S, Jansen JA, Kasper FK, Mikos AG (2012) Evaluation of bone regeneration using the rat critical size calvarial defect. Nature Protocols 7: 1918-1929.

Standal; T, Abildgaard N, Fagerli U-M, Stordal B, Hjertner O, Borset M, Sundan A (2007) HGF inhibits BMP-induced osteoblastogenesis:possible implicatios for the bone disease of multiple myeloma. Blood 109:3024-3030.

Stevenson S (1999) Biology of bone grafts. Orthop Clin North Am 30:543-552.

Stocum DL (2012) Regenerative Biology and Medicine, 2nd ed. Elsevier/Academic Press, San Diego, 465 pp.

Suckow MA, Voytik-Harbin SL, Terril LA, Badylak SF (1999) Enhanced bone regeneration using porcine small intestinal submucosa J Investig Surg 12:277-287.

Tabin CJ (2006) The key to left-right asymmetry. Cell 127:27-32.

Tolli H, Kujala S, Jamsa T, Jalovaara P (2011) Reinderr bone extract can heal the critical-size rat femur defect. Internatl Orthopaed (SICOT) 35:615-622.

Tatsumi R, Anderson E, Nevoret CJ, Halevy O, Allen RA (1998) HGF/SF is present in normal adult skeletal muscle and is capable of activating satellite cells. Dev Biol 194:114-128.

Ulmanen MS, Pekkarinen T, Hietala OA, Birr EA, Jalovaara P (2005) Osteoconductivity of partially purified native ostrich (*Struthio camelus*) bone morphogenetic protein:comparison with mammalian species. Life Sci 77:2425-2437.

Viateau V, Guillemin G, Bousson V, et al. (2007) Long-bone critical size defects treated with tissue-engineered grafts: a study on sheep. J Orthopaed Res 25:741-749.

Xu CC, Chan RW, Weinberger DG, Efune G, Pawlowski KS (2010) Controlled release of hepatocyte growth factor from a bovine acellular scaffold for vocal fold reconstruction. J Biomed Mater Res A 93:1335-1347.

Yun Y-R, Won JE, Jeon E, Lee S, Kang W, Jo H, Jang J-H, Shin US, Kim H-W (2010) Fibroblast growth factors: biology, function, and application for tissue regeneration. J Tiss Eng 2010:1-18.

Table 1: Growth factors implicated by bioinformatic analysis in cartilage and bone regeneration, and in fracture repair.

Growth Factor	Fracture Repair	Cartilage Regeneration	Bone Regeneration
FGF-2	+	+	+
PDGF-A	+	+	+
HGF	+	+	+
TGF-β 1, 2	+	+	+
TGF-β3	+	+	+
Lefty-2	+	+	+
EGF	+	-	+
PDGF B	+	-	+
PDGF D	+	-	+
VEGF A	-	+	+
Follistatin	+	-	-

Table 2: Growth factor combinations and concentrations used to induce cartilage regeneration across 50% defects in the axolotl fibula.

Treatment Group	GF Concentration	# of limbs
1. Amphibian PBS	---	10
2. BMP-4	10 ng/µl	10
VEGF	25 ng/µl	
3. BMP-4	10 ng/µl	10
HGF	10 ng/µl	
4. BMP-4	10 ng/µl	10
VEGF	25 ng/µl	
HGF	10 ng/µl	
5. BMP-4	10 ng/µl	10
VEGF	25 ng/µl	
HGF	10 ng/µl	
FGF-2	8 ng/µl	
6. BMP-4	10 ng/µl	10
VEGF	25 ng/µl	
HGF	25 ng/µl	
FGF-2	8 ng/µl	
EGF	10 ng/µl	
TGFβ-3	2ng/µl	
PDGF-AA	10 ng/µl	
7. Blastema protein extract	7µg/µl	10
8. Limb protein extract	6µg/µl	10

Table 3: Regeneration of cartilage in the absence of intervention across defects of 10%, 20%, 40% and 50% in the axolotl fibula. Fracture data is two months post-operation; 10%, 20%, 40% and 50% data is three months post-operation.

Defect Type	**Regeneration (# of Limbs)**
Fracture	12/12
10%	8/10
20%	7/8
40%	0/8
50%	0/10

Table 4: Number of limbs in which growth factors and limb tissue extract induced partial or significant/complete regeneration across 50% defects in the axolotl fibula at three months post-operation. Partial regeneration means that a small amount of cartilage/bone regenerated from one or both cut ends of the fibula. Significant regeneration means that skeletal regeneration spanned more than 50% of the defect.

	Partial Regeneration	**Significant Regeneration**
Seven Factors	1/12	0/12
BMP-4/VEGF	2/12	0/12
BMP-4/HGF	1/12	4/12
Limb Tissue Extract	2/12	4/12

Legends for Figures

Fig. 1: Juvenile adult axolotls. Left, wild-type. Right, the white mutant.
Fig. 2: 10% and 20% defects imaged by X-ray (top) and micro-CT (bottom) at two months post-operation. In the X-ray photos, the tibia is to the left and the fibula to the right in the 10% group and the tibia is to the left and the fibula to the right in the 20% group. Faint shadows indicating bone formation can be seen in the X-ray photos. In the micro-CT photos, the tibia is to the top and the fibula at the bottom. Bone formation has taken place.
Fig. 3: Whole mounts of control 10% (top) and 20% defects (bottom) stained with methylene blue (A, D) or methylene blue/alizarin red (B, E), and H & E-stained sections(C, F), two months post-operation without intervention. Tibia is on the left and fibula on the right in all photos. Both cartilage and bone have regenerated across the defects.
Fig. 4: Control 40% (A, C) and 50% (C, D) defects three months post-operation. A, B, whole mounts stained with methylene blue/alizarin red. C, D, H & E-stained sections. No regeneration has taken place. In the sections, muscle and connective tissue have filled the defect space (arrows).
Fig. 5: Bone volume fraction of regenerated bone in 105-50% defects at two months post-operation. The 20% defect is the same one illustrated in Fig. 2. Top, red dashed lines show the cross-section level of the 10% and 20% defects (A, B) and the 40% and 50% defects (C, D) where the measurements were taken. Both 10% and 20% defects regenerated a high volume fraction of bone, whereas there was much less regeneration in the 40% defects, and minimal regeneration in the 50% defects, which only regenerated at the cut ends of the fibula.
Fig. 6: Use of two fluorochromes to measure bone regeneration in 10% and 50% segment defects after 3 weeks of regeneration. 1% calcein was injected on the day of surgery at a dose of 15ug/mg body weight. 2% alizarine complexone red was injected 1 week post-surgery at a dose of 30ug/mg body weight. Samples were harvested 3 weeks post-surgery. Left (A-1,A-2,A-3) is a 10% defect; right (B-1,B-2,B-3) is a 50% defect. (A-1, B-1), calcein green fluorescence. (A2, B2), alizarine complexone red fluorescence. (A-3, B-3), red and green color merged. In the merged image of the 10% defect (A-3), the red color extends beyond the green, indicating that regeneration is taking place. By contrast, red and green show only minimal separation in the merged image of the 50% defect (B-3), indicating minimal regeneration. The extent of regeneration was obtained by measuring the length of red extending beyond green on the anterior, middle and posterior points of the anterior-posterior axis of the fibula and averaging the three measurements (bar graph).
Figure 7: Left, 8-braid scaffold prior to hydration. Middle and right, 50% defect at one and two months, respectively, after embedding SIS scaffold alone. No cartilage has regenerated. In the one-month specimen, the implanted scaffold is still visible within the gap (arrow). At two months, the scaffold is largely degraded, and connective tissue and muscle has regenerated into the gap (arrow).
Fig. 8. Left: 50% fibular defect treated with BMP4/VEGF/HGF/FGF2/PDGF-AA/TGFβ-3, three months post-implant. A small amount of regenerated cartilage was present at the proximal end of the fibula (arrow). The distal end of the fibula was severely angled with respect to the proximal end. A small amount of cartilage appears to have regenerated transversely on the distal fibula stump (asterisk). Right: 50% defect treated with BMP4/VEGF, three months post-operation. An irregular tongue of cartilage with periosteal bone collar (arrow) has regenerated from the distal end of the fibula. In both cases, remnants of the SIS scaffold can be seen within the defect, along with muscle and connective tissue.
Fig. 9: Left, MB-stained whole mount of 50% defect treated with BMP4/HGF, 3 months post-operation. A short cone of cartilage (arrow) regenerated from the proximal end of the fibula. No regeneration took place from the distal end. Right, another MB-stained whole mount of 50% defect treated with BMP4/HGF in which short cones of cartilage regenerated from both the proximal and distal ends of the fibula (arrows). Both specimens illustrate a common phenomenon encountered after removal of 50% of the bone, namely that the remaining distal and/or proximal bone segments regress to create closer to an 80% gap.
Fig. 10. Two 50% defects treated with BMP4/HGF, three months post-operation. Left, an irregular secondary length of cartilage (asterisk) was induced along the axis of the tibia (T). Vertical lines indicate the boundaries of the gap in the fibula. No skeletal tissue was regenerated within the defect space itself. except for a nodule of cartilage. Right, cartilage (asterisk) from the distal end of the fibula regenerated across 80% of the defect.
Fig. 11. Left, another example of a 50% defect three months after treatment with BMP4/HGF. Cartilage (arrow) has regenerated across the defect space. Right, 50% defect three months after treatment with tissue extract. There was extensive cartilage and bone regenerated (arrow) at an angle from the distal end of the fibula.
Fig. 12: Left, methylene blue-stained whole mount of a 50% defect three months after treatment with tissue extract. The gap has been completely bridged by cartilage, which appears to have regenerated primarily from the distal end of the fibula, with only a sliver regenerating from the proximal end (arrow). A cartilage bridge (asterisk) also formed to connect the regenerating fibula to the tibia (T). Right, Methylene blue/alizarin red-stained whole mount of a 50% defect three months after treatment with tissue extract. The ends of the fibula were angled with respect to one another, and a supernumerary foot (asterisk) regenerated perpendicular to the limb. Bone appears to have regenerated between the supernumerary foot and the proximal end of the fibula. The distal end of the fibula is indicated by the arrow.
Fig. 13. Profile of release kinetics of BMP4 from 8-braid and tubular SIS scaffolds. Release at 2 h was higher for the braid scaffold, but two days, there was no difference between the two types of scaffold.
Fig. 14: Immunohistochemistry of cartilage tissue. (A) BMP4/HGF: anti BMP4B; (B) BMP4/HGF: anti HGF. The signal for both BMP4 and HGF was strong. (C) Control, no signal.
Fig. 15: Immunohistochemistry of cartilage. (A) BMP4/VEGF: anti BMP4; (B) BMP4/VEGF: anti-HGF; (C) BMP4 negative control; (D) HGF negative control
Fig. 16: (A) TE: anti-BMP4; (B) TE: anti HGF. There is strong signal in each case.